applied sciences

MDPI

Article

Reduction of Phase Shifters in Planar Phased Arrays Using Novel Random Subarray Techniques

Juan L. Valle [1,†], Marco A. Panduro [1,*,†], Carlos del Río Bocio [2], Carlos A. Brizuela [1] and David H. Covarrubias [1]

[1] Center for Scientific Research and Higher Education at Ensenada (CICESE), Carr. Tijuana-Ensenada 3918, Zona Playitas, Ensenada 22860, Mexico; jlvalle@cicese.edu.mx (J.L.V.); cbrizuel@cicese.edu.mx (C.A.B.); dacoro@cicese.mx (D.H.C.)
[2] Electrical, Electronic and Communication Engineering, Public University of Navarre (UPNA), 31006 Pamplona, Spain; carlos@unavarra.es
* Correspondence: mpanduro@cicese.mx
† These authors contributed equally to this work.

Abstract: Reducing the number of phase shifters by grouping antenna elements into subarrays has been extensively studied for decades. The number of phase shifters directly affects the cost, complexity, and power consumption of the system. A novel method for the design of phased planar antenna arrays is presented in this work in order to perform a reduction of up to 70% in the number of phase shifters used by the array, while maintaining the desired radiation characteristics. This method consists of creating fusions of subarrays to generate random sequences that form the best feeding network configuration for planar phased arrays. The obtained solution allows scanning the mainlobe at $\theta = -40^\circ$ elevation with a range of scanning of $[-75^\circ < \phi < 75^\circ]$ in the azimuth plane, while maintaining a side lobe level below -10 dB and achieving a reduction of 62% in the number of phase shifters. It is shown that each solution is created based on search criteria, which influence the morphology of the array in terms of subarray size and orientation. The proposed methodology shows great flexibility for creating new phased antenna array designs that meet the requirements of specific applications in a short period of time.

Keywords: beamforming; planar array; phase shifter; randomized algorithm; subarray

Citation: Valle, J.L.; Panduro, M.A.; del Río Bocio, C.; Brizuela, C.A.; Covarrubias, D.H. Reduction of Phase Shifters in Planar Phased Arrays Using Novel Random Subarray Techniques. *Appl. Sci.* **2024**, *14*, 5917. https://doi.org/10.3390/app14135917

Academic Editors: Paulo M. Mendes, Carlos Lima and Hugo Daniel da Costa Dinis

Received: 4 June 2024
Revised: 29 June 2024
Accepted: 3 July 2024
Published: 6 July 2024

1. Introduction

Phased antenna arrays provide enhanced performance and flexibility compared to traditional single-element antennas, with the capability of steering and shaping their radiation patterns by combining multiple individual antenna elements [1]. This allows transmitting and receive signals in specific directions, which makes them a crucial component of modern communication systems. Planar phased arrays are currently used in a broad spectrum of beamforming applications, due to their ability to steer a beam in both azimuth and elevation planes, which makes this technology suitable for 5G and satellite applications [2,3]. Furthermore, there are applications that require almost a free redirection of the mainlobe radiant energy, such as in automotive radars and landing systems [4].

The reduction of phase shifters in the array is an important consideration in antenna design, given that phase shifters directly affect the cost, complexity, and power consumption of the system. One approach involves exploiting the spatial properties of the antenna array to achieve beamforming. This can be achieved by using subarrays [5–8], where each subarray consists of a group of antennas with a single phase shifter. Proper configuration of the subarrays allows reducing the number of phase shifters, while maintaining beamforming capabilities and achieving a complementary reduction in the side lobe level (SLL).

Previous works on the subject suggested different design techniques for planar phased arrays, such as the ones mentioned in [9–11], where distinct strategic arrangements of antenna elements into subarrays are presented. The subarrays are depicted as tiles that

form diverse geometric figures, which in some cases form a unique pattern of design. As mentioned in [12], an exhaustive methodology is used to generate various planar array designs based on the replication of geometric patterns of subarrays, which reduces the quantity of solutions in the search space. Although this approach considerably reduces the number of phase shifters in the system, there is limited scanning of the mainlobe in the elevation plane.

There have been many techniques based on subarrays in previous works, although more research is required to generate better techniques that achieve phased antenna systems with lower complexity and maintaining the desired radiation features. This paper presents a novel method for the design of phased planar antenna arrays to reduce the number of phase shifters used in the antenna system. This method consists of creating fusions of subarrays to generate random sequences that construct the best feeding network configuration with previously defined radiation characteristics for planar antenna arrays.

The techniques presented in this work can result in a reduction of up to 70% in the number of phase shifters used by the array system with respect to the conventional case of one phase shifter per antenna element. The obtained solution allows scanning the mainlobe at $\theta = -40^\circ$ elevation with a range of scanning of $[-75^\circ \leq \phi \leq 75^\circ]$ in the azimuth plane, while maintaining a side lobe level below -10 dB and achieving a reduction of 62% in the number of phase shifters. This methodology may be of interest for antenna designers in order to set appropriate design compromises between the number of control ports and radiation performance.

2. Random Subarray Design Methodology

The array factor for the planar array is defined as a function of θ and ϕ by

$$AF(\theta, \phi) = \sum_{n=1}^{N} \sum_{m=1}^{M} I_{n,m} e^{j[kd(n-1)\psi_x + kd(m-1)\psi_y + \beta_x + \beta_y]}, \quad (1)$$

where

$$\psi_x = \sin\theta + \cos\phi \quad (2)$$

$$\psi_y = \sin\theta + \sin\phi \quad (3)$$

$$\beta_x = -kd(n-1)\sin\theta_0 \cos\phi_0 \quad (4)$$

$$\beta_y = -kd(m-1)\sin\theta_0 \sin\phi_0. \quad (5)$$

The planar array consists of N columns and M rows, with a total number of $N \times M$ antennas. The separation between antenna elements is given by $d = 0.5\lambda$ and the amplitude of the nm-th antenna element is represented by $I_{n,m}$. The steering vectors β_x and β_y denote the cophasal excitation values in the x-axis and y-axis, respectively. In this work, the section of RF (radio frequency) hosts the phase shifters.

2.1. Planar Array as Matrix of Integers

As mentioned in [13], a linear array with subarrays can be represented as an array of integers (sequence), where each integer corresponds to the number of antenna elements in a given subarray K of size j, and then the number of phase shifters PS_m or subarrays per row is given by

$$PS_m = \sum_{j \in J \subset \mathbb{N}} K_j, \quad (6)$$

where $m \in [1, 2, \ldots, M-1, M]$ denotes the m-row in the array and J the subset of natural numbers that compose the different sizes of subarrays K_j.

Therefore, a matrix of $PS_m \times M$ integers is used to represent the configuration of the planar array, where PS_m represents the number of subarrays per row m and M the number of rows, where each row can be visualized as a linear array of K_j number of subarrays, as

shown in Figure 1. The total number of phase shifters used by the planar array is calculated by the sum of all subarrays in the array, such as

$$PS_{total} = \sum_{m=1}^{M} PS_m. \tag{7}$$

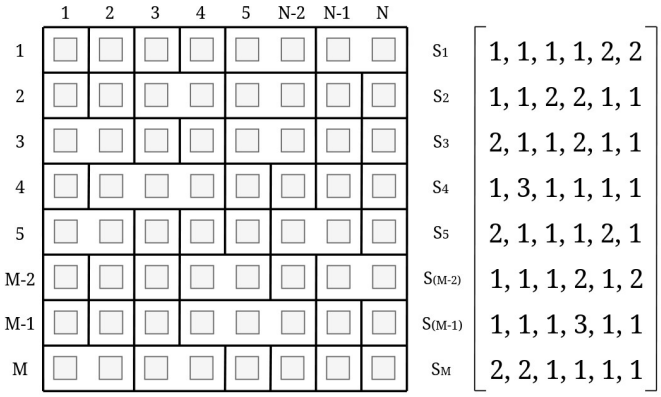

Figure 1. Representation of a 8×8 planar array as a matrix of integers with $PS_m \times M$ subarrays (6×8). Each row or sequence in the array is denoted by $\{S_m \mid m \in [1, 2, \ldots, M-1, M]\}$.

2.2. Planar Array Design from Optimal Linear Arrays

An initial approach for addressing this problem is creating a planar array from a collection of linear arrays with subarrays. These sequences are optimal solutions of an exhaustive search performed in a search space of solutions created from a given set of subarrays K_j and a steering angle usually in the range of $[-12^\circ \leq \theta \leq 12^\circ]$ for optimal performance [14].

Let S_m be a linear array that constructs each row of a $N \times M$ planar array, where $m \in [1, 2, \ldots, M-1, M]$ represents the number of rows in the array. Then, the search space $\mathcal{S}$ or number of possible solutions is defined by

$$\mathcal{S} = \frac{(s + M - 1)!}{M!(s-1)!}, \tag{8}$$

where s denotes the number of sequences used to construct each row of the planar array. When a set of subarrays of sizes j is chosen, the number of possible combinations in which a sequence can be created is given by

$$s = \frac{(PS_m)!}{\prod\limits_{j \in J \subset \mathbb{N}} (K_j)!}, \tag{9}$$

PS_m is the number of subarrays according to (6).

2.3. Phase Distribution and Operating Frequency

Phase distribution refers to the phase shift applied to the signal in each element of the array. It plays an essential role in determining the direction of the main beam and side lobes of the antenna pattern. In the case of subarrays, the overall phase distribution of the antenna array is determined by the combination of the phase shifters within each subarray and the phase shifters controlling the entire array.

Although the physical fabrication of the resultant array is outside of the scope of this work, it is intended to be a microstrip patch antenna composed of a substrate material and planned to be used as part of a cognitive radio system XCVR for satellite communications operating in the Ku-band with a downlink signal in the 10.7–12.7 GHz radio spectrum [15]. In addition, the radio system is intended to integrate a cognitive motor that employs machine learning algorithms for proper allocation of spectrum channels and accurate angle

of arrival (AoA) estimation based on closed-loop adjustments of the adaptive complex weights of the digital beamforming network.

The cognitive radio approach to channel allocation allows keeping track of the physical location of the users in the network and canceling interference from other sources present, while sensing the spectrum for user assignment in a desired real-time scenario [16]. Thus, there is a need for adequate artifact corrections, in order to reduce the number of phase errors caused by unwanted time-delays inserted into the RF circuit by means of mutual coupling, or fabrication errors in the length of the signal paths [17].

2.4. Fusions of Subarrays

A novel technique called *fusion of subarrays* is introduced in this work to reduce the number of phase shifters by combining two or more adjacent subarrays into a new subarray with more antenna elements and a new phase distribution. The idea behind this methodology is to randomize the process of creating new subarrays with geometric figures based on tiles, to reorder the grouping of the antenna elements in an initial configuration of a planar array.

In order to construct an initial $N \times M$ planar array composed of M rows, where each row corresponds to a linear array of integers, a starting sequence with a fixed number of subarrays of size K_j is randomly shuffled M times to create each row of the matrix. This allows each row to contain the same number of subarrays K_j but in random positions, ensuring $PS_m \times M$ dimensions of the array. Then, a search for adjacency between subarrays with index i_{S_m} is performed, and if this condition is met, a new fusion with probability P may occur.

$$i_{S_m} \in [1, 2, \ldots, PS_m - 1, PS_m] \tag{10}$$

For the purpose of this work, the phase distribution in the fusioned subarrays is dictated by the previously assigned distribution of phase, starting from the subarray with the lowest row in the fusion and alternating with an upper row each time fusion is performed. This means that every time a fusion happens, it is necessary to trace the past index used as reference, in order to assign a different phase each time. The intention behind this is to have an equitable distribution of phases across the array. An example of the pseudo code for this method is shown in Algorithm 1.

Algorithm 1: Pseudo code for the algorithm of Fusions of Subarrays

```
seq = [1,1,1,1,2,2];                          // initialize seed sequence //
N = M = sum(seq);                              // sum all elements in seq //
PS_m = length(seq);
for m < M/2 do
    S_(m) = shuffle(seq);                      // shuffle subarray order //
    S_(m+1) = shuffle(seq);
    for i_Sm < PS_m do
        P = random(0,1);                       // random number between 0 and 1 //
        rand = 0.75;                           // 75% of fusion //
        if P < rand then
            align-indices(i_Sm, i_Sm+1);       // check for contiguous indices //
            fusion(S_m, S_m+1, i_Sm, i_Sm+1);
            dnm(i_Sm, i_Sm+1);                 // compute new avg distances //
        else
            align-indices(i_Sm, i_Sm+1);
        end
    end
end
Inm(dnm);                                      // compute raised cosine //
AF(θ, φ, Inm);                                 // compute array factor //
```

2.4.1. Two-Row Fusion

This case requires that the number of antenna elements per row, represented by M, is an even number such that $(M \bmod 2) = 0$. The later is because each subarray fusion happens between a pair of rows, e.g., $(S_1, S_2), (S_3, S_4), \ldots, (S_{M-1}, S_M)$. Restriction of the size of each subarray $j \in [1, 2]$ is required to make every fusioned subarray restricted to a maximum of 4 antenna elements per subarray, following a design criterion for linear arrays mentioned in [13].

The fusion of two subarrays contiguously located between rows happens with a probability of P and considering that subarrays with indices i_{S_m} and $i_{S_{m+1}}$ have at least one antenna element adjacent between them. This allows expanding the size of the subarrays up to $j \in [2, 3, 4]$ after fusion has been performed.

For example, let $S_1 = [1, 1, 1, 1, 2, 2]$ and $S_2 = [1, 1, 2, 2, 1, 1]$ be a pair of rows that form a section of a planar array composed of a set of sequences $(S_1, S_2, \ldots, S_m)$, as shown in Figure 2. The fusions of subarrays happen on indices $(i_{S_1}, i_{S_2} = 1, 3)$ and indices $(i_{S_1} = 5, i_{S_2} = 4)$, but cannot be attainable for $(i_{S_1}, i_{S_2} = 5)$ due to the separation between antenna elements in both rows.

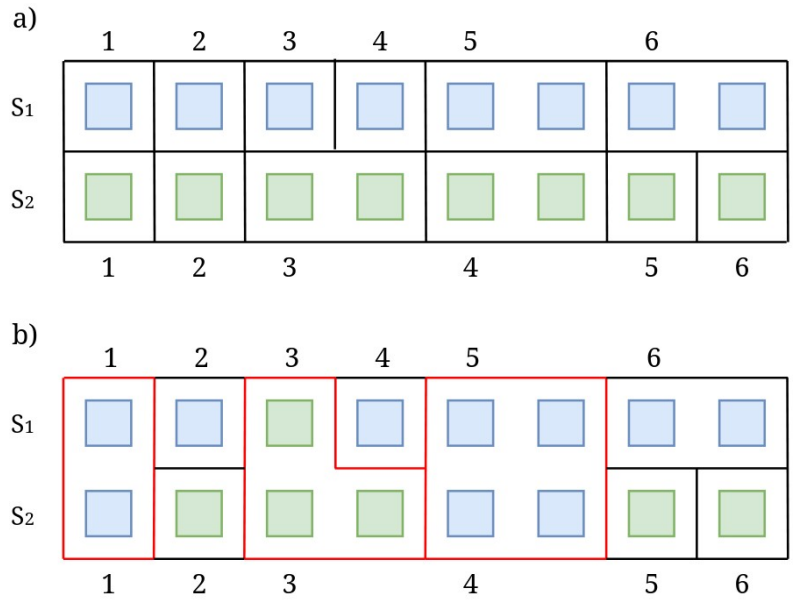

Figure 2. An illustration of the fusion of subarrays process in 2 rows: (**a**) The sequences of subarrays K_j are presented as $S_1 = [1, 1, 1, 1, 2, 2]$ with phase distribution marked in blue, and $S_2 = [1, 1, 2, 2, 1, 1]$ with phase distribution marked in green. (**b**) Resultant subarrays with three fusions performed. A new phase distribution is assigned to the fusioned subarrays.

2.4.2. Three-Row Fusion

This case is similar to the previous case, with the option of incorporating a third row into the fusion process. This means that if a first fusion occurs between two rows, a second fusion may occur if the current total number of antenna elements in the new subarray complies with the restriction of size previously stated and if the probability condition is met. This process adds more diversity to the geometric figures and reduces the number of subarrays K_j per row, which also reduces the number of phase shifters used by the array system.

Let $S_2 = [1, 1, 2, 2, 1, 1]$ and $S_3 = [2, 1, 1, 2, 1, 1]$ be the new pair of rows chosen to perform a fusion, as shown in Figure 3. The fusions of subarrays happen on indices $(i_{S_2}, i_{S_3} = 1, 3, 5)$, while maintaining the condition of size of the subarrays at $j \in [2, 3, 4]$. A new phase distribution is assigned based on choosing a different phase alternating with the last fusions performed.

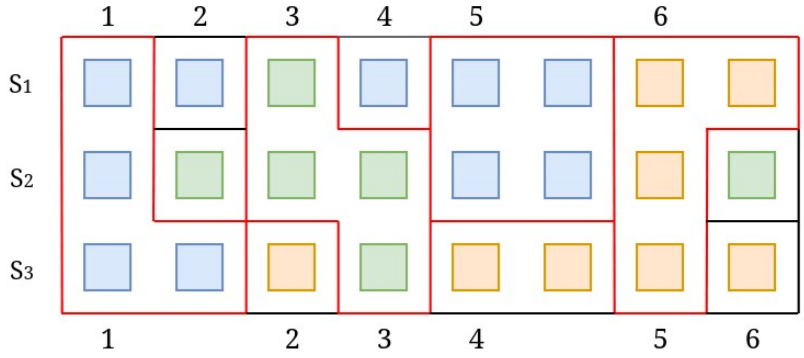

Figure 3. Example of a three-row fusion between the two-row fusion result shown in Figure 2 and a third row $S_3 = [2, 1, 1, 2, 1, 1]$. New fusions of subarrays happen on indices $i_{S_3} = 1, 3, 5$. In addition, a new phase distribution is set for the resultant array.

2.4.3. Greedy Fusion Approach

This instance of the problem eliminates the randomness of each fusion event and necessitates accomplishing every possible fusion in the array given a set of random sequences of subarrays in each row. One of the main advantages of this approach is the reduction of the search space, given that only one solution exists for each initial configuration of K_j subarrays. The number of phase shifters reduces approximately to

$$PS_{total} \approx (PS_m \times M)/2. \tag{11}$$

For example, suppose that $K_2 = 8$ are all the subarrays in the array, then there is only one solution for this instance of the problem with $8 \times 16 = 128$ phase shifters before the fusion process and $128/2 = 64$ subarrays after a greedy approach, considering that every tried fusion is successful. This results in a reduction of 75% in the number of phase shifters due to (11) in comparison with the conventional case.

2.5. Raised Cosine Tapering

Consider that the array center serves as the phase reference and $d_{n,m}$, the distance from the origin to the antenna element located at the n-column and m-row. Then, the raised cosine tapering function is given by

$$I_{n,m} = \frac{1 + \cos(\frac{d_{n,m} \cos^{-1}(2a-1)}{0.5L})}{2}, \tag{12}$$

where L represents the array longitude and $a = 0.14$ according to [18], due to the symmetry of the array. Hence,

$$d_{n,m} = \sqrt{dx_{n,m}^2 + dy_{n,m}^2}, \tag{13}$$

corresponds to the distances from the origin of the array to the antenna elements in the x and y axes. Then, $d_{n,m}$ can be treated as the hypotenuse of a right triangle with $dx_{n,m}$ and $dy_{n,m}$ as its cathetos.

Each subarray has a distance $di_{n,m}$ to the center of the planar array given by (13) as shown in Figure 4; therefore, a new average distance $d_{n,m}$ is calculated by computing the sum of the distances of each subarray involved in the fusion process divided by the number of rows R that contain those subarrays. Hence,

$$d_{n,m} = \frac{\sum_{i=1}^{R} di_{n,m}}{R}. \tag{14}$$

This can be visualized as the calculation of the centroid of the new geometric figure created from the fusion of subarrays.

a)

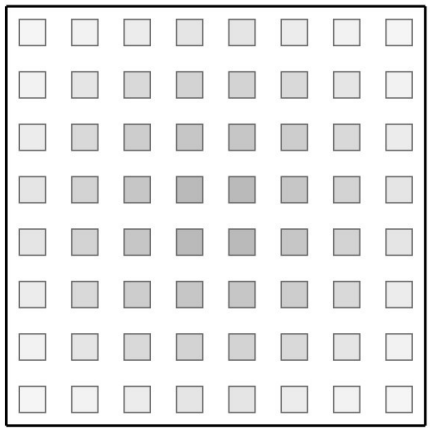

b)

0.01	0.09	0.19	0.26	0.26	0.19	0.09	0.01
0.09	0.26	0.44	0.55	0.55	0.44	0.26	0.09
0.19	0.44	0.68	0.83	0.83	0.68	0.44	0.19
0.26	0.55	0.83	1.00	1.00	0.83	0.55	0.26
0.26	0.55	0.83	1.00	1.00	0.83	0.55	0.26
0.19	0.44	0.68	0.83	0.83	0.68	0.44	0.19
0.09	0.26	0.44	0.55	0.55	0.44	0.26	0.09
0.01	0.09	0.19	0.26	0.26	0.19	0.09	0.01

Figure 4. An illustration of the amplitudes per antenna in a 8×8 planar array by applying a raised cosine tapering function. (**a**) Grey color gradient of amplitudes per antenna element. (**b**) Normalized values of the raised cosine function. Notice that the amplitude in each antenna element decreases progressively as it moves away from the center location of the array.

3. Simulation Results

This section presents the results obtained for each case previously described. An algorithm programmed in R was used to perform various instances of the problem of the design of a 16×16 phased planar antenna array. All cases were run on a *Linux Debian 12* computer (Waltham, MA, USA) system with 8 processors *Intel Core i7-8565U @ 1.80GHz* and 16*GB* of RAM (Santa Clara, CA, USA).

The elevation plane with range $[-\pi/2 \leq \theta \leq \pi/2]$ is represented by the x-axis on each graph using a resolution of $\pi/36{,}000$ points. The y-axis corresponds to the normalized array factor calculated by

$$y = 20 \log 10 \left(\frac{|AF|}{\max(|AF|)} \right). \tag{15}$$

For each case, a solution had three restrictions that had to be satisfied in order to qualify as a candidate solution, such as the ones presented in this section; starting with a minimum reduction in phase shifters or the number of fusions. Then, the performance of each array configuration was measured using a threshold value of SLL scanning at broadside or $[\theta, \phi] = [0^\circ, 0^\circ]$. Finally, the mainlobe was scanned into a desired elevation angle θ and measurement of a new SLL threshold was performed with every step angle addition $\Delta\phi$ in the azimuth plane given the desired scanning range for ϕ.

3.1. Case I: Planar Array Design from Optimal Linear Arrays

An initial number of 8 sequences was used from a Pareto front compromising SLL and FNBW, which resulted from an exhaustive search of a linear phased array with 16 antenna elements and 8 subarrays scanning at $\theta = 12^\circ$ with an SLL threshold of -10 dB. The number of possible solutions for this instance of the problem was given by the search space calculated by (8) and (9). Hence,

$$\mathcal{S} = \frac{(8 + 16 - 1)!}{16!(8 - 1)!} = 245{,}157. \tag{16}$$

Consider that each solution was computed in an average time of 0.7696 s. Therefore, an exhaustive search of the whole search space was attainable in approximately 52.41 h.

Instead of searching through all possible solutions, a random approach was used to search for a solution with SLL below -28 dB scanning at broadside in $[\theta, \phi] = [0^\circ, 0^\circ]$. Moreover, there was the capability of a maximum scanning of $\theta = 60^\circ$ in elevation and

a scanning range of $[30^\circ \leq \phi \leq 150^\circ]$ in azimuth with a step angle of $\Delta\phi = 15^\circ$, while maintaining a SLL below -10 dB.

The number of phase shifters used by the array could be calculated in advance due to the fixed number of 8 subarrays per row, therefore $PS_{total} = 8 \times 16 = 128$ according to (7). This ensured a reduction of 50% of the phase shifters used in the conventional case, where a phase shifter is used for each antenna element in the array.

A solution that satisfied the search criteria was obtained after 197 iterations with a computational time of 2.53 min. The planar array is illustrated in Figure 5, with SLL levels for each scanning angle in ϕ shown in Table 1.

Table 1. Results of SLL and FNBW for the planar phased array shown in Figure 5.

ϕ	*SLL* (dB)	FNBW (rad.)	Color
30°	−10.11	1.4142	Red
45°	−12.74	1.2269	Green
60°	−16.45	1.3133	Magenta
75°	−22.91	0.8407	Cyan
90°	−26.35	1.1809	Orange
105°	−25.54	0.8523	Yellow
120°	−15.47	1.3314	Blue
135°	−13.70	0.8332	Pink
150°	−10.09	0.8132	Aqua

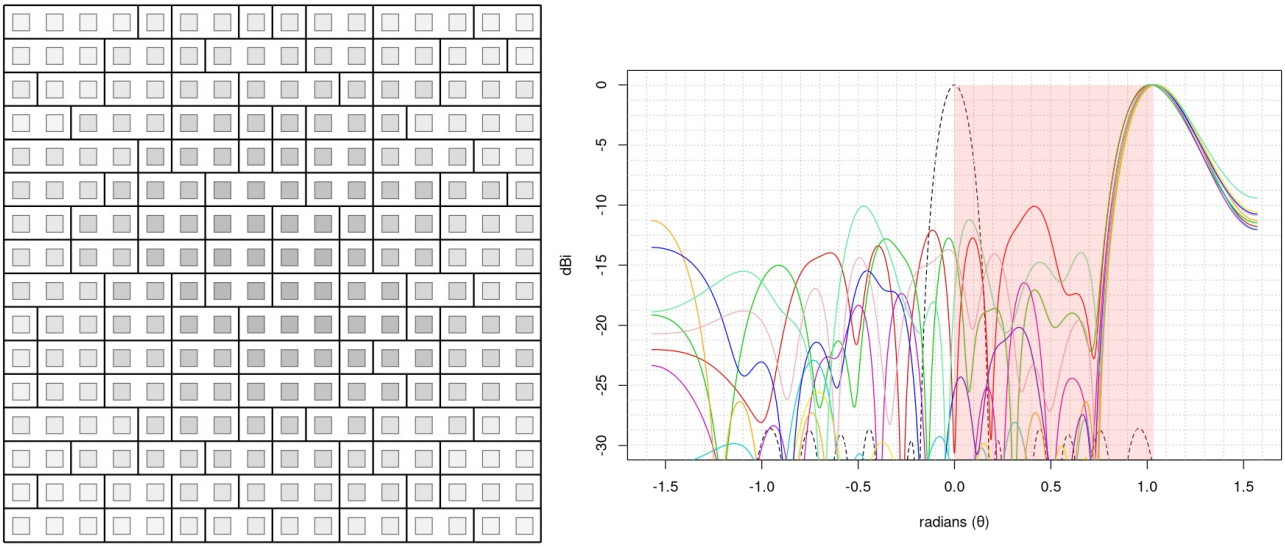

Figure 5. Radiation pattern and design of the planar phased array obtained in Case I. The natural response is shown in black dotted lines. The scanning range in the elevation plane is illustrated by the red rectangle ($0^\circ \leq \theta \leq 60^\circ$) with an azimuth scanning range of $[30^\circ \leq \phi \leq 150^\circ]$. The color palette for different radiation patterns indicates each step angle $\Delta\phi$ shown in Table 1.

3.2. Case II: Greedy Fusions of Subarrays in 2 Rows

In order to reduce the number of phase shifters used by the array to near 75%, according to (11), a greedy approach was performed for this instance of the problem. Each sequence for a row was created randomly using subarrays of size $K_1 = 6$ and $K_2 = 5$, and a maximum number of 4 antenna elements per subarray was allowed after a successful fusion.

For this case, the search criteria were to find a solution with a natural response in broadside below -25 dB scanning at $[\theta, \phi] = [0^\circ, 0^\circ]$ and a scanning capability of $\theta = 60^\circ$ in elevation and $[-20^\circ \leq \phi \leq 20^\circ]$ in azimuth, with a step angle of $\Delta\phi = 10^\circ$, while maintaining a SLL below -10 dB.

A reduction of 69% in the number of phase shifters with respect to the conventional case was accomplished using this approach. The solution shown in Figure 6 was found after 1576 iterations with a total computational time of 12.64 min.

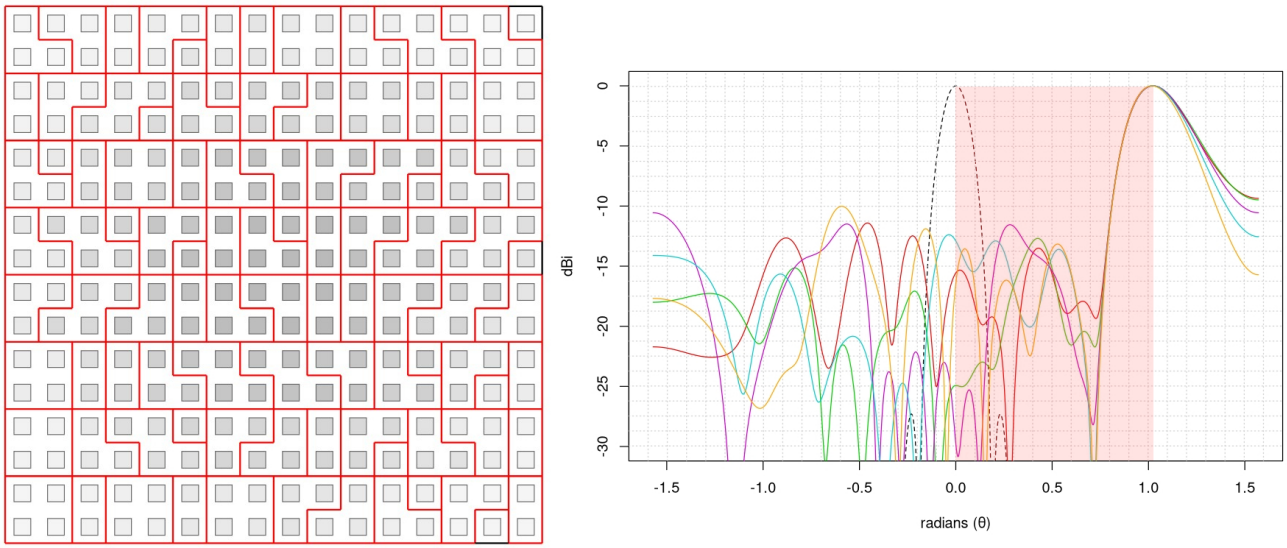

Figure 6. Radiation pattern and design of the planar phased array obtained in Case II. The natural response is shown in black dotted lines. The scanning range in the elevation plane is illustrated by the red rectangle ($0° \leq \theta \leq 60°$) with an azimuth scanning range of $[-20° \leq \phi \leq 20°]$. The color palette for different radiation patterns indicates each step angle $\Delta\phi$ shown in Table 2.

Table 2. Results of SLL and FNBW for the planar phased array shown in Figure 6.

ϕ	*SLL* (dB)	FNBW (rad.)	Color
$-20°$	-11.41	1.1480	Red
$-10°$	-12.69	0.8492	Green
$0°$	-11.49	1.2844	Magenta
$10°$	-12.38	1.3229	Cyan
$20°$	-10.02	1.4058	Orange

3.3. Case III: Fusions of Subarrays in 3 Rows

An initial condition of $K_1 = 1, K_2 = 3, K_3 = 3$ was used to randomly create solutions with 112 initial subarrays. In this case, an additional row was added to the fusion process. This time, a combination of the greedy approach and a restriction of 6 antenna elements per subarray was introduced in order to keep some of the arrays out of the fusion process, with the latter to generate disturbances in terms of the variables used that might enrich the design process.

The search criteria for this case corresponded to a natural response in broadside below -25 dB scanning at $[\theta, \phi] = [0°, 0°]$ with an elevation angle of $\theta = -40°$ and a scanning range of $[75° \leq \phi \leq 120°]$ in the azimuth plane, with a step angle of $\Delta\phi = 15°$ and a SLL below -10 dB.

A reduction of 70% in the number of phase shifters was accomplished by using this technique. The solution illustrated in Figure 7 was found after 17,602 iterations, with a total computational time of 2.45 h.

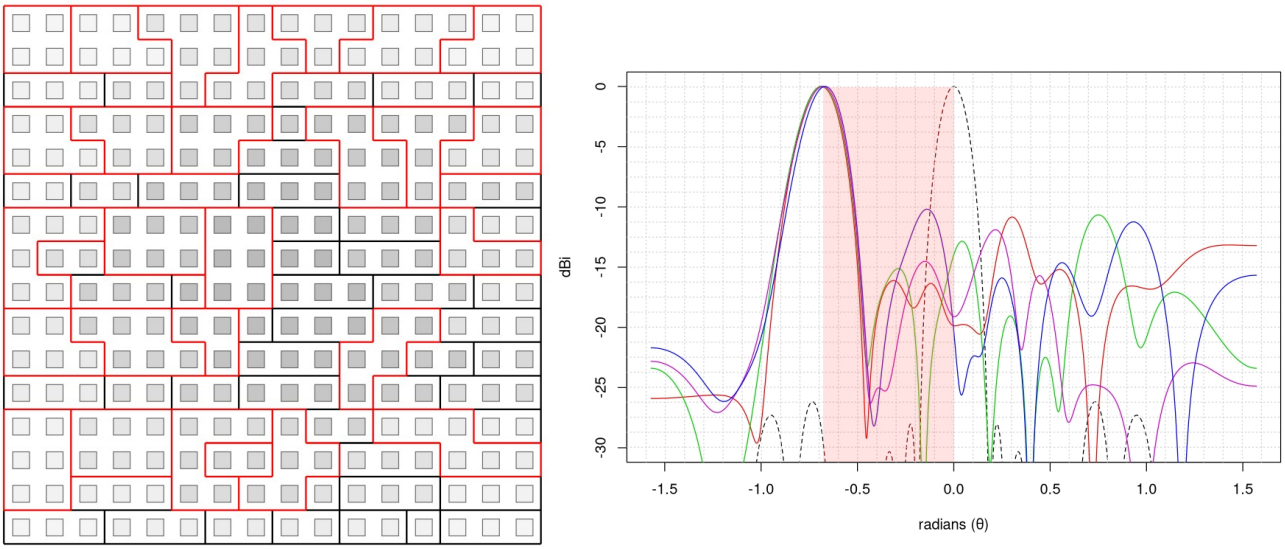

Figure 7. Radiation pattern and design of the planar phased array obtained in Case III. The natural response is shown in black dotted lines. The scanning range in the elevation plane is illustrated by the red rectangle ($-40° \leq \theta \leq 0°$) with an azimuth scanning range of $[75° \leq \phi \leq 120°]$. The color palette for different radiation patterns indicates each step angle $\Delta\phi$ shown in Table 3.

Table 3. Results of SLL and FNBW for the planar phased array shown in Figure 7.

ϕ	*SLL* (dB)	FNBW (rad.)	Color
75°	−10.84	0.5694	Red
90°	−10.66	0.7566	Green
105°	−11.90	0.7962	Magenta
120°	−10.19	0.7789	Blue

3.4. Case IV: Fusions of Subarrays with Mixed Techniques

This case demonstrated the potential capabilities of all the techniques previously discussed but mixed together. The search criteria for the planar array were to scan the mainlobe at $\theta = -40°$ in elevation with a range of scanning of $[-75° < \phi < 75°]$ in azimuth, with a step angle of $\Delta\phi = 15°$ while maintaining the SLL below -10 dB.

A new approach was introduced by reducing the probability of fusion to zero for antenna elements in columns $6 < n < 11$ and rows $6 < m < 11$, and the last row that was not fusionable was inserted at $m = 6$. The latter was due to the advantages of having subarrays of size $j \in [1, 2]$ near the center of the array. In this case, each fusion could contain up to 6 antenna elements per subarray, and the probability of fusion used for the 2nd row was 75% and a probability of 90% for the 3rd row.

The design of the planar array obtained for this case is illustrated in Figure 8. This solution was obtained after 8351 iterations with a computational time of 1.20 h. A reduction of 62% in the number of phase shifters was accomplished assuring a scan range of the mainlobe of 150° in the azimuth plane and 40° in the elevation plane.

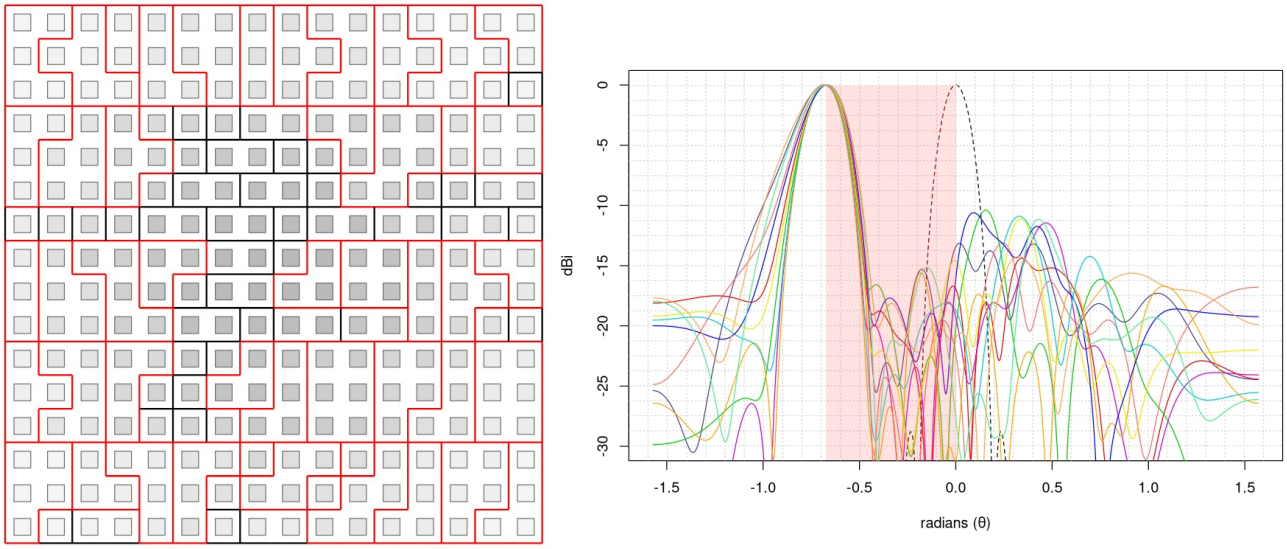

Figure 8. Radiation pattern and design of the planar phased array obtained in Case IV. The natural response is shown in black dotted lines. The scanning range in the elevation plane is illustrated by the red rectangle ($-40^\circ \leq \theta \leq 0^\circ$) with an azimuth scanning range of $[-75^\circ \leq \phi \leq 75^\circ]$. The color palette for different radiation patterns indicates each step angle $\Delta\phi$ shown in Table 4.

Table 4. Results of SLL and FNBW for the planar phased array shown in Figure 8.

ϕ	*SLL* (dB)	FNBW (rad.)	Color
-75°	-13.14	0.9498	Purple
-60°	-13.11	1.7294	Pink
-45°	-14.39	0.6319	Red
-30°	-10.40	0.5891	Green
-15°	-11.45	0.5184	Magenta
0°	-15.61	0.5397	Orange
15°	-10.90	0.5496	Cyan
30°	-11.11	0.6428	Yellow
45°	-10.61	0.7880	Blue
60°	-11.15	0.7891	Aqua
75°	-14.24	0.8223	Beige

4. Discussion and Conclusions

A novel method for the design of phased planar antenna arrays was presented in this work, in order to perform a reduction of up to 70% in the number of phase shifters used by the array, while maintaining the desired radiation characteristics. This method consists of creating fusions of subarrays to generate random sequences that construct the best feeding network configuration for planar phased arrays. It was shown that each solution was created based on search criteria that influenced the morphology of the array in terms of subarray size and orientation. This also could be visualized using the grey gradient, which showed the smoothness provided by the raised cosine function amplitudes of each subarray and its contribution to the whole array.

One of the main reasons for choosing a random approach for the search algorithms is that the number of solutions in each case increases to an intractable number. Consider that for Case I depicted in Section 3.1 there was an exhaustive search time of approximately two days, which is attainable in terms of computational time. However, as mentioned in Case II (Section 3.2), the execution time increases exponentially due to the number of different possible rows (462) that can be created randomly from a set of given subarrays due to (9). Then, the number of possible solutions is given by

$$\mathcal{S} = \frac{(462 + 16 - 1)!}{16!(462 - 1)!} \approx 2.662 \times 10^{29}. \tag{17}$$

To overcome this, computational intelligence in the form of evolutionary algorithms was applied to the search of solutions that satisfy diverse instances of the phased array design problem by partially exploring massive spaces of solutions [14,19–21].

The designs mentioned in Sections 3.3 and 3.4 illustrate the various applications of the planar phased arrays, given a set of design variables that are generally defined by the main task of the application, such as tracking the orbit of a satellite given a desired scan range [22] or an automotive application [13]. This diversity of solutions is shown in Table 5, with the comparison of Case IV of this work with other cases. The methodology presented in this work showed great flexibility in searching for new phased antenna array designs that met the requirements of an specific application in a short period of time.

Table 5. Comparison of Case IV from Section 3.4 with other cases mentioned in previous works.

Case	Number of Antenna Elements	Number of Phase Shifters	Reduction in Phase Shifters	Scan Range in Elevation (θ)	Scan Range in Azimuth (ϕ)	Higher SLL (dB)
Case IV	256	97	62%	$-40°$	$-75°$ to $75°$	-10.40
Results in [4]	16	1	92%	$0°$	$\pm 50°$	≈ -16
Figure 9 in [10]	432	12	97%	$23°$	$0°$	-16.50
Case I in [12]	256	76	70%	$-40°$	$0°$ to $90°$	≈ -10
Sec. III in [13]	30	12	60%	$\pm 14°$	$0°$	≈ -15
Config. 3 in [18]	49	15	69%	$\pm 25°$	$\pm 25°$	≈ -19
Results in [23]	64	16	75%	$\pm 25°$	$\pm 50°$	≈ -18

Author Contributions: Conceptualization, C.A.B.; Methodology, J.L.V. and M.A.P.; Software, J.L.V.; Validation, J.L.V. and C.d.R.B.; Formal analysis, J.L.V. and D.H.C.; Investigation, J.L.V. and M.A.P.; Resources, M.A.P. and C.d.R.B.; Writing – original draft, C.A.B. and J.L.V.; Writing – review & editing, C.d.R.B. and C.A.B.; Supervision, M.A.P.; Project administration, D.H.C.; Funding acquisition, D.H.C. All authors have read and agreed to the published version of the manuscript.

Funding: This research received no external funding.

Institutional Review Board Statement: Not applicable.

Informed Consent Statement: Not applicable.

Data Availability Statement: The original contributions presented in the study are included in the article, further inquiries can be directed to the corresponding author.

Conflicts of Interest: The funders had no role in the design of the study; in the collection, analyses, or interpretation of data; in the writing of the manuscript; or in the decision to publish the results.

References

1. Mailloux, R.J. *Phased Array Antenna Handbook*; Artech House: Boston, MA, USA; London, UK, 2017.
2. Vallappil, A.K.; Rahim, M.K.A.; Khawaja, B.A.; Murad, N.A.; Mustapha, M.G. Butler matrix based beamforming networks for phased array antenna systems: A comprehensive review and future directions for 5G applications. *IEEE Access* **2020**, *9*, 3970–3987. [CrossRef]
3. Wang, C.; Wang, Y.; Lian, P.; Xue, S.; Xu, Q.; Shi, Y.; Jia, Y.; Du, B.; Liu, J.; Tang, B. Space phased array antenna developments: A perspective on structural design. *IEEE Aerosp. Electron. Syst. Mag.* **2020**, *35*, 44–63. [CrossRef]
4. Ku, B.H.; Schmalenberg, P.; Inac, O.; Gurbuz, O.D.; Lee, J.S.; Shiozaki, K.; Rebeiz, G.M. A 77–81-GHz 16-Element Phased-Array Receiver with $\pm 50°$ Beam Scanning for Advanced Automotive Radars. *IEEE Trans. Microw. Theory Tech.* **2014**, *62*, 2823–2832. [CrossRef]
5. Haupt, R. Reducing grating lobes due to subarray amplitude tapering. *IEEE Trans. Antennas Propag.* **1985**, *33*, 846–850. [CrossRef]
6. Goffer, A.P.; Kam, M.; Herczfeld, P.R. Design of phased arrays in terms of random subarrays. *IEEE Trans. Antennas Propag.* **1994**, *42*, 820–826. [CrossRef]
7. Xiong, Z.Y.; Xu, Z.H.; Chen, S.W.; Xiao, S.P. Subarray partition in array antenna based on the algorithm X. *IEEE Antennas Wirel. Propag. Lett.* **2013**, *12*, 906–909. [CrossRef]
8. Juárez, E.; Panduro, M.A.; Reyna, A.; Covarrubias, D.H.; Mendez, A.; Murillo, E. Design of concentric ring antenna arrays based on subarrays to simplify the feeding system. *Symmetry* **2020**, *12*, 970. [CrossRef]
9. Rocca, P.; Mailloux, R.; Toso, G. GA-based optimization of irregular subarray layouts for wideband phased arrays design. *IEEE Antennas Wirel. Propag. Lett.* **2014**, *14*, 131–134. [CrossRef]

10. Krivosheev, Y.V.; Shishlov, A.V.; Denisenko, V.V. Grating lobe suppression in aperiodic phased array antennas composed of periodic subarrays with large element spacing. *IEEE Antennas Propag. Mag.* **2015**, *57*, 76–85. [CrossRef]
11. Rocca, P.; Anselmi, N.; Polo, A.; Massa, A. Modular design of hexagonal phased arrays through diamond tiles. *IEEE Trans. Antennas Propag.* **2020**, *68*, 3598–3612. [CrossRef]
12. Rupakula, B.; Aljuhani, A.H.; Rebeiz, G.M. Limited scan-angle phased arrays using randomly grouped subarrays and reduced number of phase shifters. *IEEE Trans. Antennas Propag.* **2019**, *68*, 70–80. [CrossRef]
13. Avser, B.; Pierro, J.; Rebeiz, G.M. Random feeding networks for reducing the number of phase shifters in limited-scan arrays. *IEEE Trans. Antennas Propag.* **2016**, *64*, 4648–4658. [CrossRef]
14. Valle, J.L.; Brizuela, C.A.; Panduro, M.A.; Reyna, A. Reduction of the number of phase shifters in linear phased antenna arrays by using evolutionary multi-objective optimization. In Proceedings of the 2019 IEEE International Symposium on Antennas and Propagation and USNC-URSI Radio Science Meeting, Atlanta, GA, USA, 7–12 July 2019, pp. 55–56.
15. Humphreys, T.E.; Iannucci, P.A.; Komodromos, Z.M.; Graff, A.M. Signal structure of the Starlink Ku-band downlink. *IEEE Trans. Aerosp. Electron. Syst.* **2023**, *59*, 6016–6030. [CrossRef]
16. Haykin, S.; Thomson, D.J.; Reed, J.H. Spectrum sensing for cognitive radio. *Proc. IEEE* **2009**, *97*, 849–877. [CrossRef]
17. Florio, A.; Avitabile, G.; Coviello, G. A Linear Technique for Artifacts Correction and Compensation in Phase Interferometric Angle of Arrival Estimation. *Sensors* **2022**, *22*, 1427. [CrossRef] [PubMed]
18. Juárez, E.; Panduro, M.A.; Covarrubias, D.H.; Reyna, A. Coherently radiating periodic structures to reduce the number of phase shifters in a 2-D phased array. *Sensors* **2021**, *21*, 6592. [CrossRef] [PubMed]
19. Boeringer, D.W.; Werner, D.H. Particle swarm optimization versus genetic algorithms for phased array synthesis. *IEEE Trans. Antennas Propag.* **2004**, *52*, 771–779. [CrossRef]
20. Khodier, M.M.; Christodoulou, C.G. Linear array geometry synthesis with minimum sidelobe level and null control using particle swarm optimization. *IEEE Trans. Antennas Propag.* **2005**, *53*, 2674–2679. [CrossRef]
21. Panduro, M.A.; Brizuela, C.A.; Balderas, L.I.; Acosta, D.A. A comparison of genetic algorithms, particle swarm optimization and the differential evolution method for the design of scannable circular antenna arrays. *Progress Electromagn. Res.* **2009**, *13*, 171–186. [CrossRef]
22. Cakaj, S. The parameters comparison of the "Starlink" LEO satellites constellation for different orbital shells. *Front. Commun. Netw.* **2021**, *2*, 643095. [CrossRef]
23. Nafe, A.; Sayginer, M.; Kibaroglu, K.; Rebeiz, G.M. 2×64-Element Dual-Polarized Dual-Beam Single-Aperture 28-GHz Phased Array With 2×30 Gb/s Links for 5G Polarization MIMO. *IEEE Trans. Microw. Theory Tech.* **2020**, *68*, 3872–3884. [CrossRef]